DEUTSCHES ELEKTRONEN-SYNCHROTRON DESY

DESY 74/61
January 1975

Electroproduction of η Mesons in the Region of the Resonance $S_{11}(1535)$

by

J.-C. Alder, F.W. Brasse, W. Fehrenbach, J. Gayler, R. Haidan, G. Glöe, S.P. Goel, V. Korbel, W. Krechlok, J. May, M. Merkwitz, R. Schmitz, W. Wagner

2 HAMBURG 52 · NOTKESTIEG 1

To be sure that your preprints are promptly included in the
HIGH ENERGY PHYSICS INDEX ,
send them to the following address (if possible by air mail) :

DESY
Bibliothek
2 Hamburg 52
Notkestieg 1
Germany

Electroproduction of η Mesons in the Region of the Resonance $S_{11}(1535)$

J.-C. Alder[1], F.W. Brasse, W. Fehrenbach[2], J. Gayler, R. Haidan, G. Glöe[3], S.P. Goel, V. Korbel[4], W. Krechlok, J. May, M. Merkwitz, R. Schmitz and W. Wagner[5]

ABSTRACT

We report on an experiment on electroproduction in the resonance region in the mass range $1505 \leq W \leq 1715$ MeV. Data have been taken at $q^2 = 0.22$, 0.6 and 1 GeV^2. The obtained angular distributions support that η production proceeds mainly through S-wave excitation due to the resonance $S_{11}(1535)$.

The total cross section of the formation of this resonance decreases much more slowly with increasing momentum transfer than the total ep cross section.

Now at:
1) Université de Lausanne
2) BABCOCK-Brown Boveri Reaktor GmbH., Mannheim
3) T Ü V, Hamburg
4) CERN, Genf
5) PHILIPS, Hamburg

INTRODUCTION

The available data on electron-nucleon scattering do not yet allow to disentangle the different contributions of the various baryon resonances to the total ep cross section. However, two resonances can be studied fairly independently from all the others, the resonances $P_{33}(1236)$ and $S_{11}(1535)$. The resonance $P_{33}(1236)$ dominates π^o production at low energies and has been studied in several experiments[1-5].

Since only the resonance $S_{11}(1535)$ has a large branching ratio to the decay channel ηp, this resonance can be isolated by the investigation of the reaction $ep \rightarrow ep\eta$.

It has been shown by Kummer et al.[6] that the cross section of the reaction $ep \rightarrow ep\eta$ at W = 1.53 GeV decreases remarkably slowly with increasing momentum transfer. Beck et al.[7] found in an experiment where the η was measured only near the electron scattering plane that the differential cross section is rather independent of the polar CMS production angle Θ^* up to $q^2 = 0.4\ GeV^2$.

The present experiment covers a wider range in solid angle and W. The decay angular distributions are analysed in terms of angular coefficients as a function of W. First results of this experiment have been reported at the Bonn Conference 1973[8].

NOTATION

We express the cross sections in terms of the virtual photon absorption cross section $d\sigma/d\Omega_\eta^*$ in the CMS of the final hadrons which is related to the differential coincidence cross section $d^5\sigma/dE'\, d\Omega_e\, d\Omega_\eta^*$ by the virtual photon flux factor Γ_t (defined as usually[2])

$$\frac{d^5\sigma}{dE'\, d\Omega_e\, d\Omega_\eta^*} = \Gamma_t \frac{d\sigma}{d\Omega_\eta^*} \quad . \tag{1}$$

If the assumption holds that in the final state only contributions of S-wave, interference of S-wave with P-wave and P-wave with total angular momentum 1/2 are present, the differential cross section can be described by[9]

$$\frac{d\sigma}{d\Omega^*} = A_o + \varepsilon B_o + (A_1 + \varepsilon B_1)\cos\theta^* + D_o \sqrt{2\varepsilon(\varepsilon+1)}\sin\theta^*\cos\Phi \qquad (2)$$

The coefficients A_o through D_o are functions of W, the invariant mass of the final ηp system, and the momentum transfer q^2 only.

The angles θ^* and Φ are the CMS polar and azimuthal production angles of the η meson (see fig. 1). The parameter ε describes the polarization of the virtual photon, e.g.[2].

If the reaction proceeds entirely through S-wave, the cross section reduces to

$$\frac{d\sigma}{d\Omega^*} = A_o + \varepsilon B_o. \qquad (3)$$

In this case there is no scalar-transverse interference term (D_o). Therefore the presence of scalar excitation of the resonances $S_{11}(1535)$ can only be demonstrated by variation of ε, which was not done in this experiment.

APPARATUS

The measurements are done in an external e^- beam of DESY. The primary beam hits a 12 cm liquid hydrogen target (fig. 2). The intensity is controlled by a secondary emission monitor, which was compared many times during the experiment to a Faraday cup.

The scattered electron is detected in a double focussing and vertically bending spectrometer[10] with momentum resolution of $\Delta p/p \sim 0.5$ %, vertical angle resolution of ~ 4 mr and horizontal angle resolution of ~ 2.7 mr. The total acceptances are $\Delta p/p \sim 10$ %, $\Delta\varphi_{vert} \sim 60$ mr and $\Delta\vartheta_{hor} \sim 15$ mr. The electron is identified by a threshold CO_2-Cerenkov- and a sandwich shower counter.

The recoling proton is detected in coincidence with the scattered e^- in a nonfocussing spectrometer[11] consisting of a vertically bending dipole magnet and two hodoscopes behind it. The trajectory of a particle is defined by the target and the crossing points with the hodoscopes. The first one is a system of 3 multiple wire proportional chambers (750 wires each)[12], mea-

suring the vertical coordinate to ± 1 mm and the horizontal one to ± 12 mm. The second hodoscope consists of 76 scintillation counters vertically arranged in Gray-Code, giving 450 vertical bins (10 mm each). The horizontal coordinate is measured with phototubes on both sides of one of the coded scintillators, thus measuring the time difference between the signals of these multipliers. The horizontal resolution is 80 mm[13], the total horizontal acceptance is about 6°. The vertical angular acceptance is momentum dependent. For average momenta in this experiment it is 20°.
The information of each event is taken by a PDP 8I processor[14] on line with the IBM 360/65 at the DESY Rechenzentrum. There the data is stored on magnetic tape for off line analysis. On line the experiment is controlled by the IBM via the small processor.

DATA ANALYSIS

The secondary electron and the recoiling proton are detected in coincidence. The reaction $ep \to ep\eta$ clearly shows up in the missing mass spectrum. An example of a missing mass spectrum is given in fig. 3. Protons are distinguished from π^+ mesons by the time difference of the electron and hadron signal. Fig. 4 shows that a clear separation in the covered range of momenta is possible. Some pion background in the remaining proton sample was rejected by the requirement of sufficient pulse height of scintillator signals.

Acceptances and various corrections have been calculated by a Monte Carlo simulation of the whole experiment. The W and q^2 dependence of η production used for the simulation was taken from a preliminary analysis[8]. Radiation corrections have been incorporated into the Monte Carlo simulation including internal and external radiation. Also a multipion background has been added according to a phase space distribution. Experimental and Monte Carlo events were then analysed by the same program.

The multipion background has been subtracted from the data by the following method. First the multipion missing mass distribution obtained by the Monte Carlo simulation is fitted for each bin ($\Delta W = 30$ MeV, $\Delta \cos\Theta^* = 0.2$, $\Delta\Phi = 30^{\circ}$) in the mass range $0.24 < M^2 < 0.38$ GeV^2 with a smooth polynomial Ansatz. This leads to a function $f(M^2)$ describing the background. The experimental η yield is then determined by fitting an expression $\alpha\, f(M^2) + \beta + \gamma \cdot M^2$ to the experimental missing mass distribution of the cor-

responding bin. The 3 parameters α, β, γ in this fit are determined only by the data outside the η peak. Finally the number of the Monte Carlo η events used to calculate the cross section is determined by just the same fit to the simulated events. An example of a missing mass distribution of a particular angular bin and the obtained background is given in fig. 5 for experimental and for simulated events.

The data are corrected for empty target rate, nuclear absorption, dead time loss, inefficiencies, multi track events, random background.

RESULTS

All data have been taken with the central electron spectrometer angle set to 15°. The polarization parameter ε was always close to 0.9. The errors given in the figures are statistical only. An overall systematic error of 6% should be taken into account.

Figs. 6, 7 give some examples of the obtained angular distributions presented in table 1. There is no strong dependence on Θ^* or Φ visible in the data. All angular distributions obtained at $q^2 = 0.6$ and 1 GeV^2 have been fitted to the angular dependence of eqns. 2 and 3. The obtained χ^2 per degree of freedom is in all cases below 1.6 even with the assumption of an isotropic distribution (eqn. 3). If the S P interference terms are also included in the fit (eqn. 2) the term $A_o + \varepsilon B_o$ stays dominant. The scalar-transverse interference term D_o is consistent with zero. Up to W = 1.625 GeV the obtained standard deviations of D_o are about 10 % of $A_o + \varepsilon B_o$. Also inclusion of higher waves (terms $\sin^2 \Theta^* \cos 2\Phi$ or $\cos^2 \Theta^*$) gives no significant improvements of the fits. The angular distributions were therefore fitted with only $A_1 + \varepsilon B_1$ kept as a free parameter in addition to $A_o + \varepsilon B_o$. The data at $q^2 = 0.22$ GeV^2 are not sufficient to determine several coefficients independently. Therefore the coefficient $A_1 + \varepsilon B_1$ has been fixed to zero in this case. The solid lines in figs. 6, 7 represent these fits to all the data of one W-q^2 bin not only to the data shown in the figures.

The obtained angular coefficients are presented in fig. 8 and table 2 as function of W.

The total cross section

$$\sigma_{tot} = 4\pi \quad (A_o + \varepsilon B_o)$$

as a function of W can be represented (fig. 8) by the following Breit Wigner expression

$$\sigma_{tot} = \frac{\vec{p}_\eta^{\,CM}}{\vec{q}^{\,CM}} \times \frac{A}{(W-W_{Res})^2 + \Gamma(W)^2/4}$$

where, $\vec{p}_\eta$ and $\vec{q}^{\,CM}$ are the three momenta of the η meson and the virtual photon in the CM-system. The width Γ has been parametrized according to the branching ratio of the decay modes of $S_{11}(1535)$ [18].

$$\Gamma(W) = \Gamma_o \; (0.55 \times \vec{p}_\eta^{\,CM}/\vec{p}_{\eta_{Res}}^{\,CM} + 0.35 \times \vec{p}_\pi^{\,CM}/\vec{p}_{\pi_{Res}}^{\,CM} + 0.1)$$

The solid lines in fig. 8 are least square fits of the above formula to the measured cross sections with A, Γ_o and W_{Res} kept as free parameters. The obtained A, Γ_o and W_{Res} are given in table 3. In the case of $q^2 = 0.22$ GeV^2 Γ_o and W_{Res} have been fixed to the values obtained at $q^2 = 0.6$ GeV^2.

We interpret the term $A_o + \varepsilon B_o$ as an indicator of the resonance $S_{11}(1535)$. The strength of this resonance even at $q^2 = 1$ GeV^2 is remarkable. The total η production cross section at $q^2 = 1$ GeV^2 is only by about 20 % smaller than the photoproduction cross section. Assuming a partial decay rate of 55 % for $S_{11} \rightarrow \eta p$ the resonance $S_{11}(1535)$ contributes at $W = 1.535$ GeV, $q^2 = 1$ GeV^2 about 19 μb. This is more than 20 % of the total $\gamma_v p$ cross section of about 80 μb. At $q^2 = 0$ the resonance $S_{11}(1535)$ contributes at most 10 % to the total cross section. In view of the fact that the second bump in the total $\gamma_v p$ cross section stays equally prominent between $q^2 = 0$ and $q^2 = 1$ GeV^2, our results imply that the resonance $D_{13}(1520)$ decreases faster with increasing momentum transfer than the total $\gamma_v p$ cross section. The question arises whether the large cross section of $S_{11}(1535)$ at space like momentum transfer is due to scalar excitation. The present data give no information about this. A recent parton model calculation of H. Goldberg [15] favours transverse excitation.

Plotting our results together with those of other groups we find (fig. 9) that our data points are systematically higher than those of Beck et al.[7] and Kummer et al.[6]. This difference may be due to the strong W-dependence of the cross sections. Our results give the cross section at W = 1.535 GeV and not an average over a range of W values.

In fig. 9 the results are also compared with symmetric quark model calculations of Ravndal[16] and Lipes[17]. The form factor of Ravndal is not an output of the quark model. It was introduced as a reasonable assumption. The better agreement with the calculations of Lipes seems to be accidental. This model predicts the $D_{13}(1520)$ to decrease even slower than the $S_{11}(1535)$ in contradiction to the above arguments.

Acknowledgements

We thank R.C.E. Devenish and F. Gutbrod for helpful discussions.

References

1. C. Mistretta et al., Phys. Rev. 184 (1969) 1487
2. J.-C. Alder et al., Nucl. Phys. B 46 (1972) 573
   W. Albrecht et al., Nucl. Phys. B 25 (1970) 1
3. R. Siddle et al., Nucl. Phys. B 35 (1971) 93
4. S. Galster et al., Phys. Rev. D5 (1972) 519
5. K. Bätzner et al., Nucl. Phys. B76 (1974) 1
6. P.S. Kummer et al., Phys. Rev. Letters 30, 873 (1973)
7. U. Beck et al., Physics Letters 51B (1974) 103
8. J.-C. Alder et al., Contribution to the 6th International Symposium on Electron and Photon Interactions at High Energies, Bonn 1973

   A.B. Clegg, Proceedings of the 6th International Symposium on Electron and Photon Interactions at High Energies, Bonn, 1973
9. C.W. Akerlof et al., Phys. Rev. Letters 14 (1965) 1036
10. J. Gayler, Thesis, DESY F21-71/2 (1971);
    J. May, Thesis, DESY F21-71/3 (1971)
11. K.-H. Frank,DESY F21-72/1 (1972) and DESY F21-72/2 (1972)
12. G. Glöe, Diplomarbeit, Universität Hamburg (1973)
13. W. Wagner, DESY F21-73/1 (1973)
14. R. Schmitz, Diplomarbeit, Universität Hamburg (1973)
15. H. Goldberg, SLAC-PUB-1349 (1973)
16. F. Ravndal, Phys. Rev. D4 (1971) 1466
17. R.G. Lipes, Phys. Rev. D5 (1972) 2849
18. Particle Data Group, Physics Letters 50B (1974)

Table 1: Differential cross sections of the reaction $\gamma_v + p \to \eta + p$.
The errors do not contain an overall systematic error of 6 %.

$q^2 = 0.23$ GeV^2 W=1505 MeV ε=0.87

$\cos\theta^*$	Φ[°]	$d\sigma/d\Omega^*$ [µb/sr]
-0.9	115.	2.07 +- 0.50
-0.9	75.	0.75 +- 0.19
-0.9	35.	0.82 +- 0.22
-0.9	-5.	1.34 +- 0.54
-0.7	115.	1.62 +- 0.59
-0.7	75.	1.07 +- 0.19
-0.7	35.	1.29 +- 0.37
-0.5	75.	1.28 +- 0.28
-0.3	75.	1.06 +- 0.23
-0.1	75.	1.20 +- 0.23
0.1	75.	1.02 +- 0.37

$q^2 = 0.22$ GeV^2 W=1535 MeV ε= 0.86

$\cos\theta^*$	Φ[°]	$d\sigma/d\Omega^*$ [µb/sr]
-0.9	75.	1.11 +- 0.27
-0.9	35.	1.59 +- 0.37
-0.9	-5.	0.81 +- 0.37
-0.7	75.	1.36 +- 0.29
-0.7	35.	0.99 +- 0.41
-0.5	75.	1.24 +- 0.25
-0.3	75.	0.67 +- 0.37
-0.1	75.	1.21 +- 0.43
0.1	75.	0.79 +- 0.47
0.3	75.	1.65 +- 0.61

$q^2 = 0.22$ GeV^2 W=1565 MeV ε = 0.85

$\cos\theta^*$	Φ[°]	$d\sigma/d\Omega^*$ [µb/sr]
-0.9	75.	0.68 +- 0.30
-0.9	35.	0.79 +- 0.28
-0.7	75.	0.60 +- 0.25
-0.5	75.	0.74 +- 0.27
-0.1	75.	0.80 +- 0.45
0.1	75.	0.84 +- 0.51
0.3	75.	1.11 +- 0.84

$q^2 = 0.60$ GeV^2 W=1505 MeV ε = 0.91

$\cos\theta^*$	Φ[°]	$d\sigma/d\Omega^*$ [µb/sr]
-0.9	150.	1.00 +- 0.22
-0.9	120.	0.75 +- 0.18
-0.9	60.	0.76 +- 0.18
-0.9	30.	0.92 +- 0.36
-0.7	150.	0.79 +- 0.21
-0.7	120.	0.83 +- 0.15
-0.7	90.	0.76 +- 0.13
-0.7	60.	0.90 +- 0.14
-0.7	30.	0.72 +- 0.21
-0.5	150.	0.97 +- 0.24
-0.5	120.	0.93 +- 0.14
-0.5	90.	1.14 +- 0.39
-0.5	60.	0.89 +- 0.15
-0.5	30.	0.92 +- 0.18
-0.3	120.	1.17 +- 0.18
-0.3	90.	0.91 +- 0.16
-0.3	60.	0.98 +- 0.17
-0.1	120.	0.72 +- 0.15
-0.1	90.	1.00 +- 0.17
-0.1	60.	0.99 +- 0.18
0.1	120.	0.99 +- 0.28
0.1	90.	1.09 +- 0.24
0.1	60.	1.26 +- 0.20
0.3	120.	0.60 +- 0.19
0.3	90.	1.00 +- 0.29
0.3	60.	0.77 +- 0.14
0.5	120.	1.00 +- 0.28
0.5	90.	0.60 +- 0.23
0.5	60.	0.66 +- 0.21

$q^2 = 0.59$ GeV^2 W=1535 MeV ε = 0.90

$\cos\theta^*$	Φ [°]	$d\sigma/d\Omega^*$ [µb/sr]
-0.9	180.	0.77 +- 0.21
-0.9	150.	0.66 +- 0.24
-0.9	120.	0.82 +- 0.17
-0.9	90.	0.85 +- 0.18
-0.9	60.	0.85 +- 0.26
-0.9	30.	1.31 +- 0.21
-0.9	0.	1.36 +- 0.27
-0.7	150.	1.32 +- 0.48
-0.7	120.	0.99 +- 0.19
-0.7	90.	0.56 +- 0.18
-0.7	60.	1.20 +- 0.18
-0.7	30.	1.20 +- 0.22
-0.5	120.	1.06 +- 0.22
-0.5	90.	1.28 +- 0.20
-0.5	60.	1.44 +- 0.18

Table 1 (continued)

q^2 = 0.59 GeV^2 W = 1535 MeV ε = 0.90

cosθ*	Φ [°]	dσ/dΩ* [μb/sr]
-0.5	30.	1.22 +- 0.22
-0.3	120.	1.16 +- 0.22
-0.3	90.	1.04 +- 0.16
-0.3	60.	1.26 +- 0.19
-0.1	120.	1.16 +- 0.37
-0.1	90.	1.05 +- 0.18
-0.1	60.	1.41 +- 0.19
0.1	120.	0.94 +- 0.27
0.1	90.	1.46 +- 0.21
0.1	60.	0.66 +- 0.20
0.3	120.	1.86 +- 0.45
0.3	90.	1.15 +- 0.22
0.3	60.	1.04 +- 0.21
0.5	120.	1.29 +- 0.28
0.5	90.	1.47 +- 0.25
0.5	60.	1.30 +- 0.25

q^2 = 0.57 GeV^2 W = 1595 MeV ε = 0.89

cos θ*	Φ [°]	dσ/dΩ* [μb/sr]
-0.9	120.	0.41 +- 0.23
-0.9	90.	0.90 +- 0.22
-0.9	60.	0.34 +- 0.20
-0.9	30.	0.31 +- 0.15
-0.7	60.	0.91 +- 0.32
-0.7	30.	0.80 +- 0.48
-0.5	90.	0.72 +- 0.24
-0.5	60.	0.79 +- 0.17
-0.3	90.	0.87 +- 0.23
-0.3	60.	0.88 +- 0.23
-0.1	90.	0.44 +- 0.17
-0.1	60.	0.91 +- 0.26
0.1	90.	0.65 +- 0.28
0.1	60.	0.44 +- 0.22
0.3	90.	0.51 +- 0.23
0.3	60.	0.52 +- 0.22
0.5	90.	0.87 +- 0.26
0.7	90.	0.74 +- 0.25

q^2 = 0.58 GeV^2 W = 1565 MeV ε = 0.90

cosθ*	Φ [°]	dσ/dΩ* [μb/sr]
-0.9	150.	0.77 +- 0.27
-0.9	120.	0.72 +- 0.15
-0.9	90.	0.97 +- 0.17
-0.9	60.	0.94 +- 0.20
-0.9	30.	0.64 +- 0.17
-0.9	0.	1.46 +- 0.47
-0.7	120.	0.52 +- 0.19
-0.7	90.	0.82 +- 0.11
-0.7	60.	0.60 +- 0.15
-0.7	30.	0.66 +- 0.17
-0.5	120.	0.96 +- 0.37
-0.5	90.	0.56 +- 0.13
-0.5	60.	0.68 +- 0.12
-0.5	30.	0.98 +- 0.21
-0.3	90.	1.26 +- 0.18
-0.3	60.	1.20 +- 0.21
-0.1	120.	1.44 +- 0.52
-0.1	90.	0.69 +- 0.15
-0.1	60.	0.92 +- 0.15
0.1	90.	1.06 +- 0.21
0.1	60.	1.06 +- 0.22
0.3	90.	1.12 +- 0.18
0.3	60.	0.85 +- 0.18
0.5	90.	0.65 +- 0.12
0.5	60.	0.77 +- 0.19

q^2 = 0.99 GeV^2 W = 1505 MeV ε = 0.92

cosθ*	Φ [°]	dσ/dΩ* [μb/sr]
-0.9	60.	0.561 +- 0.176
-0.9	30.	1.008 +- 0.270
-0.7	60.	0.918 +- 0.175
-0.7	30.	0.853 +- 0.234
-0.5	60.	0.795 +- 0.129
-0.5	30.	0.865 +- 0.175
-0.3	90.	1.055 +- 0.298
-0.3	60.	0.896 +- 0.138
-0.3	30.	0.597 +- 0.231
-0.1	60.	0.779 +- 0.130
-0.1	30.	0.836 +- 0.242
0.1	120.	0.710 +- 0.308
0.1	60.	0.695 +- 0.147
0.3	60.	1.033 +- 0.195
0.5	60.	0.936 +- 0.175
0.5	30.	0.786 +- 0.185
0.7	60.	0.872 +- 0.171
0.7	30.	0.943 +- 0.251
0.9	60.	0.370 +- 0.252
0.9	30.	0.916 +- 0.247
0.9	0.	0.772 +- 0.354

Table 1(continued)

q^2 = 0.98 GeV^2 W = 1535 MeV ε = 0.91

cosθ*	Φ [°]	dσ/dΩ* [μb/sr]
-0.9	90.	0.660 +- 0.210
-0.9	60.	0.545 +- 0.246
-0.9	30.	0.766 +- 0.189
-0.9	0.	1.087 +- 0.263
-0.7	90.	1.155 +- 0.218
-0.7	60.	0.698 +- 0.130
-0.7	30.	0.723 +- 0.129
-0.7	0.	0.954 +- 0.254
-0.5	120.	0.734 +- 0.262
-0.5	90.	0.797 +- 0.207
-0.5	60.	0.818 +- 0.126
-0.5	30.	0.974 +- 0.150
-0.3	120.	0.682 +- 0.227
-0.3	90.	0.599 +- 0.236
-0.3	60.	0.904 +- 0.113
-0.3	30.	0.653 +- 0.176
-0.1	120.	1.130 +- 0.272
-0.1	90.	0.869 +- 0.282
-0.1	60.	0.776 +- 0.115
0.1	120.	1.022 +- 0.353
0.1	90.	0.786 +- 0.265
0.1	60.	1.008 +- 0.131
0.3	90.	0.732 +- 0.202
0.3	60.	1.093 +- 0.145
0.5	90.	0.973 +- 0.354
0.5	60.	1.008 +- 0.187
0.7	60.	0.993 +- 0.254
0.7	30.	1.084 +- 0.231
0.9	60.	0.736 +- 0.235
0.9	0.	0.884 +- 0.360

q^2 = 0.97 GeV^2 W = 1565 MeV ε = 0.91

cosθ*	φ [°]	dσ/dΩ* [μb/sr]
-0.9	180.	0.806 +- 0.225
-0.9	150.	0.720 +- 0.148
-0.9	120.	0.611 +- 0.081
-0.9	90.	0.530 +- 0.092
-0.9	60.	0.807 +- 0.171
-0.9	30.	0.622 +- 0.094
-0.9	0.	0.725 +- 0.180
-0.7	150.	1.090 +- 0.215
-0.7	120.	0.550 +- 0.083
-0.7	90.	0.673 +- 0.105
-0.7	60.	0.689 +- 0.091
-0.7	30.	0.605 +- 0.079
-0.7	0.	0.756 +- 0.189
-0.5	120.	0.801 +- 0.112
-0.5	90.	0.854 +- 0.126

q^2 = 0.97 GeV^2 W = 1565 MeV ε = 0.91

cosθ*	Φ [°]	dσ/dΩ* [μb/sr]
-0.5	60.	0.661 +- 0.069
-0.5	30.	0.651 +- 0.088
-0.3	120.	0.754 +- 0.140
-0.3	90.	0.860 +- 0.114
-0.3	60.	0.689 +- 0.071
-0.3	30.	0.794 +- 0.159
-0.1	120.	0.945 +- 0.187
-0.1	90.	0.819 +- 0.095
-0.1	60.	0.770 +- 0.077
0.1	120.	1.192 +- 0.188
0.1	90.	0.870 +- 0.111
0.1	60.	0.947 +- 0.094
0.3	120.	0.830 +- 0.266
0.3	90.	0.813 +- 0.122
0.3	60.	0.510 +- 0.093
0.5	90.	0.530 +- 0.138
0.5	60.	0.866 +- 0.119
0.7	60.	0.894 +- 0.223
0.9	60.	0.927 +- 0.269

q^2 = 0.95 GeV^2 W = 1595 MeV ε = 0.91

cosθ*	Φ [°]	dσ/dΩ* [μb/sr]
-0.9	150.	0.455 +- 0.076
-0.9	120.	0.548 +- 0.080
-0.9	90.	0.554 +- 0.079
-0.9	60.	0.407 +- 0.112
-0.9	30.	0.470 +- 0.074
-0.9	0.	0.607 +- 0.163
-0.7	120.	0.520 +- 0.075
-0.7	90.	0.611 +- 0.076
-0.7	60.	0.563 +- 0.061
-0.7	30.	0.535 +- 0.069
-0.7	0.	0.681 +- 0.133
-0.5	120.	0.500 +- 0.110
-0.5	90.	0.437 +- 0.088
-0.5	60.	0.555 +- 0.055
-0.5	30.	0.636 +- 0.098
-0.3	120.	0.475 +- 0.234
-0.3	90.	0.552 +- 0.086
-0.3	60.	0.609 +- 0.067
-0.3	30.	0.472 +- 0.104
-0.1	90.	0.553 +- 0.078
-0.1	60.	0.706 +- 0.087
0.1	120.	0.404 +- 0.162
0.1	90.	0.583 +- 0.087
0.1	60.	0.516 +- 0.068
0.3	120.	0.562 +- 0.174
0.3	90.	0.582 +- 0.077
0.3	60.	0.374 +- 0.071
0.5	90.	0.566 +- 0.122
0.5	60.	0.657 +- 0.130

Table 1 (continued)

q^2 = 0.94 GeV^2 W = 1625 MeV ε = 0.90

cosθ*	Φ [°]	dσ/dΩ* [μb/sr]
-0.9	150.	0.256 +- 0.088
-0.9	120.	0.322 +- 0.060
-0.9	90.	0.233 +- 0.066
-0.9	60.	0.246 +- 0.093
-0.9	30.	0.440 +- 0.098
-0.9	0.	0.420 +- 0.120
-0.7	120.	0.326 +- 0.096
-0.7	90.	0.332 +- 0.056
-0.7	60.	0.366 +- 0.072
-0.7	30.	0.335 +- 0.044
-0.7	0.	0.474 +- 0.105
-0.5	120.	0.339 +- 0.144
-0.5	90.	0.337 +- 0.065
-0.5	60.	0.344 +- 0.056
-0.5	30.	0.324 +- 0.053
-0.3	90.	0.361 +- 0.093
-0.3	60.	0.369 +- 0.053
-0.3	30.	0.277 +- 0.084
-0.1	90.	0.369 +- 0.104
-0.1	60.	0.382 +- 0.079
0.1	90.	0.373 +- 0.072
0.1	60.	0.265 +- 0.057
0.3	90.	0.364 +- 0.166
0.3	60.	0.202 +- 0.055
0.5	90.	0.161 +- 0.076
0.5	60.	0.195 +- 0.079

q^2 = 0.91 GeV^2 W = 1685 MeV ε = 0.89

cosθ*	Φ [°]	dσ/dΩ* [μb/sr]
-0.9	120.	0.088 +- 0.074
-0.9	90.	0.226 +- 0.071
-0.9	60.	0.172 +- 0.051
-0.9	30.	0.382 +- 0.180
-0.7	90.	0.081 +- 0.070
-0.7	60.	0.101 +- 0.079
-0.7	30.	0.230 +- 0.068
-0.7	0.	0.201 +- 0.118
-0.5	60.	0.228 +- 0.070
-0.5	30.	0.124 +- 0.047
-0.5	0.	0.410 +- 0.301
-0.3	90.	0.102 +- 0.057
-0.3	60.	0.131 +- 0.045
-0.1	90.	0.155 +- 0.070
-0.1	60.	0.084 +- 0.054
0.1	60.	0.193 +- 0.087
0.3	90.	0.276 +- 0.093
0.7	60.	1.102 +- 0.895

q^2 = 0.93 GeV^2 W = 1655 MeV ε = 0.90

cosθ*	Φ [°]	dσ/dΩ* [μb/sr]
-0.9	90.	0.226 +- 0.045
-0.9	60.	0.221 +- 0.065
-0.9	30.	0.160 +- 0.067
-0.7	120.	0.316 +- 0.136
-0.7	90.	0.193 +- 0.046
-0.7	60.	0.309 +- 0.076
-0.7	30.	0.219 +- 0.040
-0.7	0.	0.224 +- 0.081
-0.5	90.	0.241 +- 0.059
-0.5	60.	0.220 +- 0.041
-0.5	30.	0.287 +- 0.053
-0.3	90.	0.135 +- 0.060
-0.3	60.	0.220 +- 0.048
-0.1	60.	0.211 +- 0.047
0.1	90.	0.168 +- 0.072
0.1	60.	0.158 +- 0.051
0.3	90.	0.185 +- 0.083
0.3	60.	0.204 +- 0.062
0.5	60.	0.208 +- 0.067

q^2 = 0.90 GeV^2 W = 1715 MeV ε = 0.88

cosθ*	Φ [°]	dσ/dΩ* [μb/sr]
-0.9	90.	0.135 +- 0.063
-0.9	60.	0.220 +- 0.084
-0.7	90.	0.081 +- 0.063
-0.7	60.	0.130 +- 0.076
-0.7	30.	0.154 +- 0.042
-0.7	0.	0.145 +- 0.051
-0.5	0.	0.105 +- 0.091
-0.3	90.	0.080 +- 0.060
-0.3	60.	0.161 +- 0.058
-0.1	60.	0.206 +- 0.068
0.1	90.	0.112 +- 0.057
0.3	60.	0.214 +- 0.082
0.5	90.	0.291 +- 0.107
0.7	90.	0.383 +- 0.243
0.7	60.	0.236 +- 0.197

Table 2: Angular coefficients of the reaction $\gamma_v + p \to \eta + p$.
The errors do not contain an overall systematic error of 6 %.

q^2 [GeV^2]	W [MeV]	ε	$A_o + \varepsilon B_o$ [μb/sr]	$A_1 + \varepsilon B_1$ [μb/sr]
0.23	1505	0.87	1.06 ± 0.08	-
0.22	1535	0.86	1.14 ± 0.11	-
0.22	1565	0.85	0.72 ± 0.13	-
0.60	1505	0.91	0.871 ± 0.043	-0.009 ± 0.082
0.59	1535	0.90	1.176 ± 0.051	0.220 ± 0.087
0.58	1565	0.90	0.838 ± 0.043	0.078 ± 0.073
0.57	1595	0.89	0.649 ± 0.063	0.094 ± 0.107
0.99	1505	0.92	0.806 ± 0.042	0.027 ± 0.078
0.98	1535	0.91	0.884 ± 0.038	0.132 ± 0.072
0.97	1565	0.91	0.735 ± 0.026	0.095 ± 0.045
0.95	1595	0.91	0.543 ± 0.022	0.006 ± 0.038
0.94	1625	0.90	0.286 ± 0.019	-0.071 ± 0.033
0.93	1655	0.90	0.210 ± 0.019	-0.016 ± 0.033
0.91	1685	0.89	0.145 ± 0.029	-0.010 ± 0.050
0.90	1715	0.88	0.176 ± 0.026	0.056 ± 0.044

Table 3: Breit Wigner curve (see text) fitted to the data.

q^2 [GeV^2]	A [μb·GeV^2]	Γ_o [MeV]	M_{RES} [MeV]
0.23	0.173	--	--
0.6	0.215	154	1526
1	0.204	147	1524

Figure Captions

Fig. 1 Definition of angles

Fig. 2 Apparatus

Fig. 3 Distribution of missing mass squared for protons detected in coincidence with electrons.

Fig. 4 Momentum versus time of flight for protons and π^+ detected in coincidence with electrons.

Fig. 5 Example of a missing mass distribution of a particular angular bin in the case of experimental and Monte Carlo events. Solid line: fitted multipion background

Fig. 6 Angular distributions of $\gamma_v p \to \eta p$ at $q^2 = 1$ GeV^2.

Fig. 7 Same as fig. 6 in the case of $q^2 = 0.22$ GeV^2 and $q^2 = 0.6$ GeV^2

Fig. 8 Coefficients of angular distributions as function of W for $q^2 = 0.22$, 0.6 and 1.0 GeV^2.
At $q^2 = 0.22$ GeV^2 the coefficient $A_1 + \varepsilon B_1$ has been fixed to zero. Solid line: Breit Wigner curve (see text).

Fig. 9 Total cross section for $\gamma_v p \to \eta p$ at W = 1.535 GeV as function of q^2.
The error bars of our data do not contain a systematic error of 6 %.

Solid lines: quark model calculations by Ravndal[16] and Lipes[17] and the dipol form factor, all normalized to $q^2 = 0$.

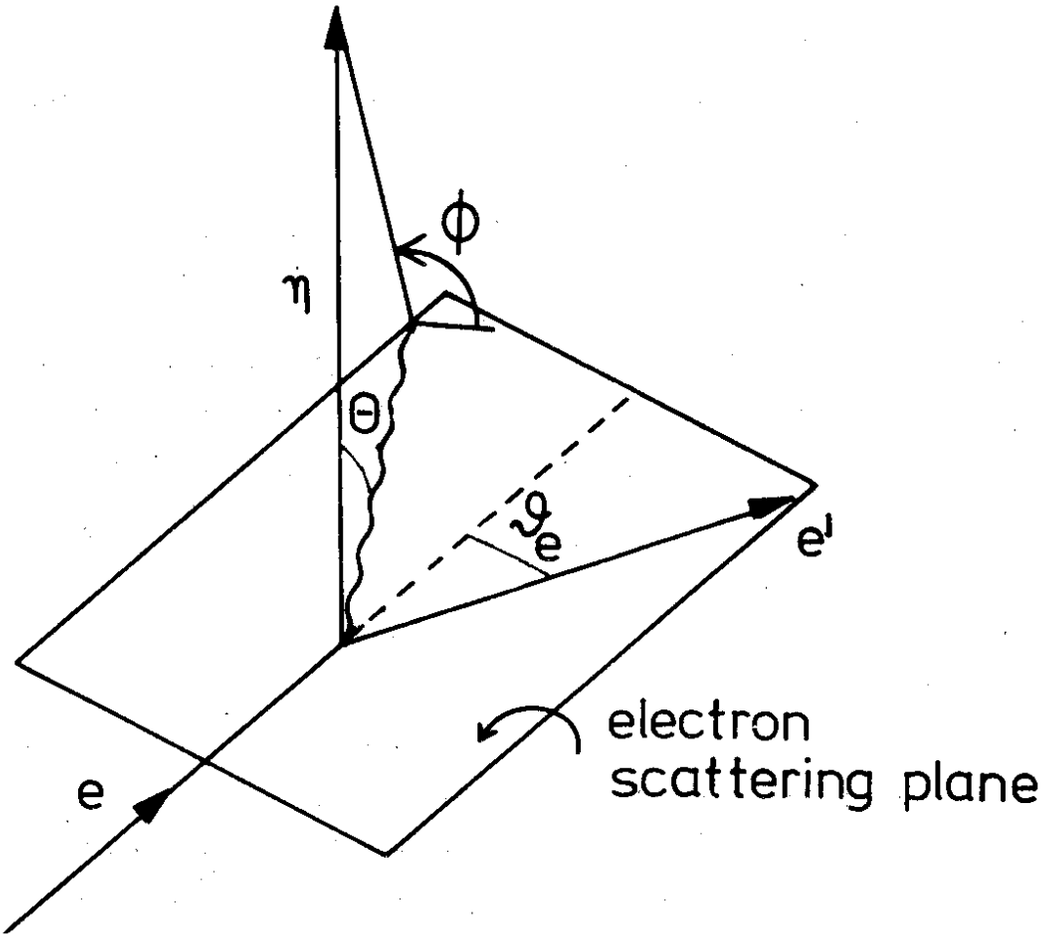

Fig. 1

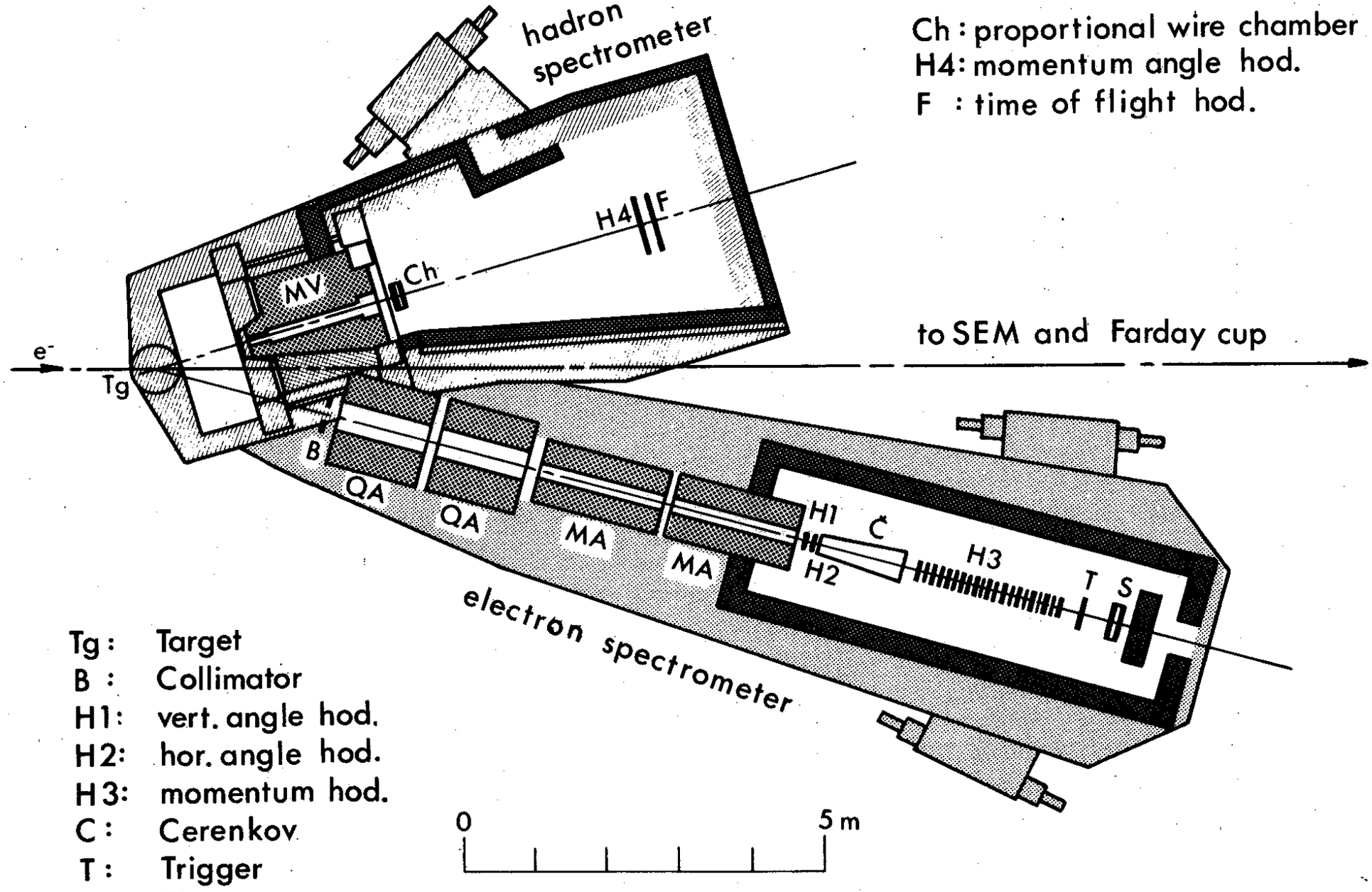
hadron spectrometer
Ch : proportional wire chamber
H4: momentum angle hod.
F : time of flight hod.
H4
F
MV
Ch
e⁻
Tg
to SEM and Farday cup
B
QA
QA
MA
MA
H1
C
H2
H3
T
S
electron spectrometer
Tg : Target
B : Collimator
H1: vert. angle hod.
H2: hor. angle hod.
H3: momentum hod.
C : Cerenkov
T : Trigger
S : Shower
0
5 m

Fig. 2

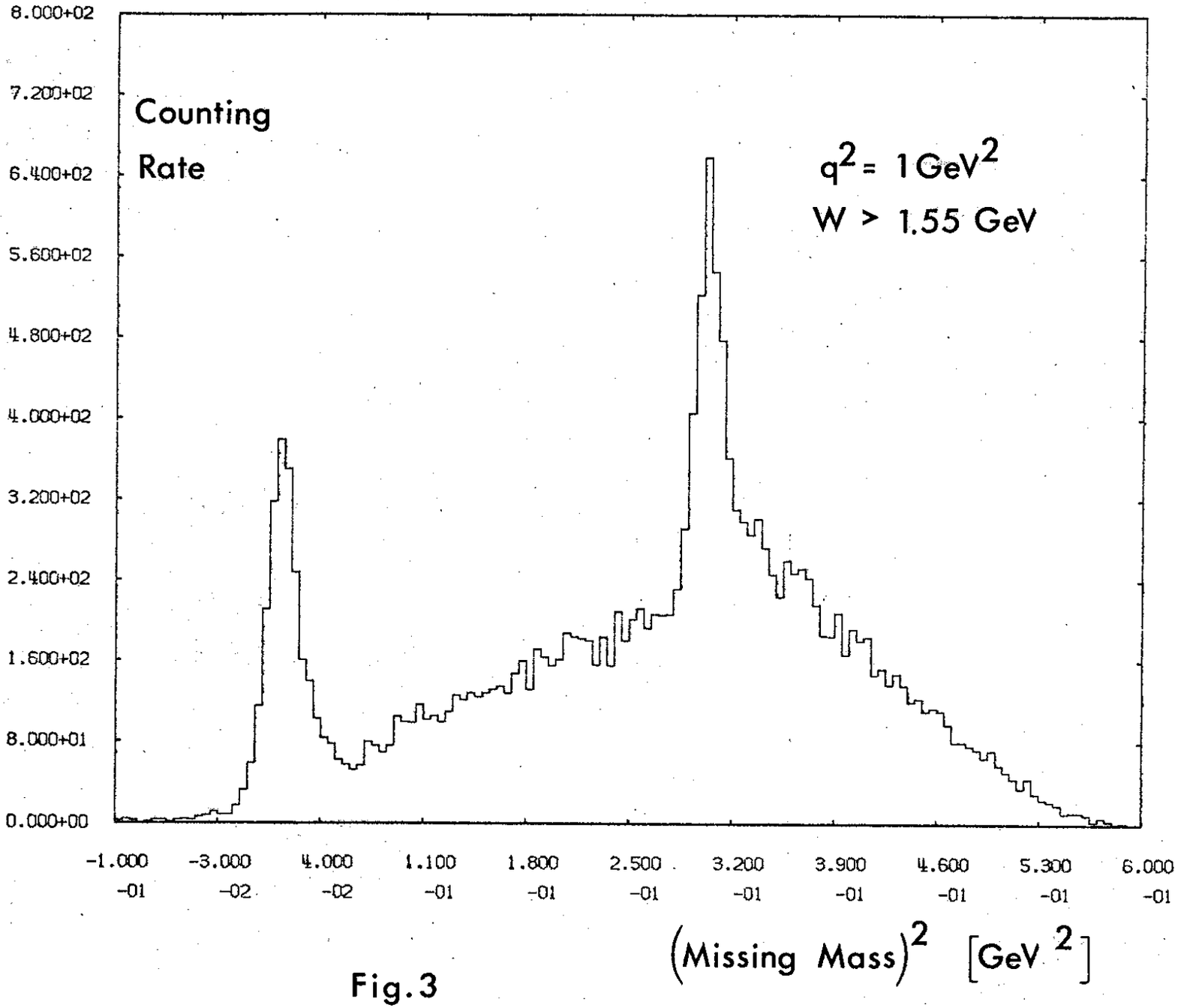
Counting
Rate
$q^2 = 1 GeV^2$
W > 1.55 GeV
8.000+02
7.200+02
6.400+02
5.600+02
4.800+02
4.000+02
3.200+02
2.400+02
1.600+02
8.000+01
0.000+00
-1.000 -01
-3.000 -02
4.000 -02
1.100 -01
1.800 -01
2.500 -01
3.200 -01
3.900 -01
4.600 -01
5.300 -01
6.000 -01
$(Missing\ Mass)^2\ [GeV^2]$

Fig.3

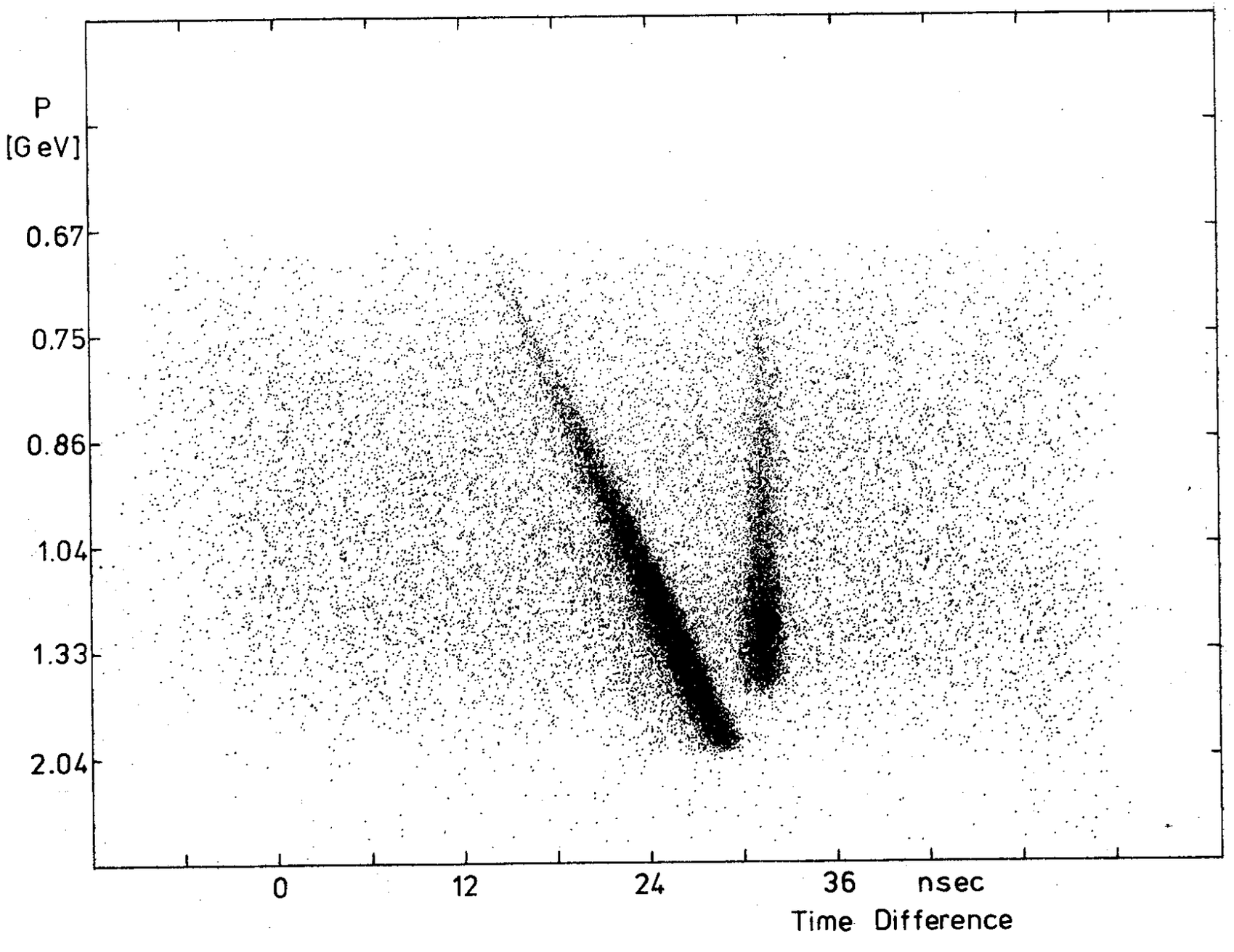

Fig. 4

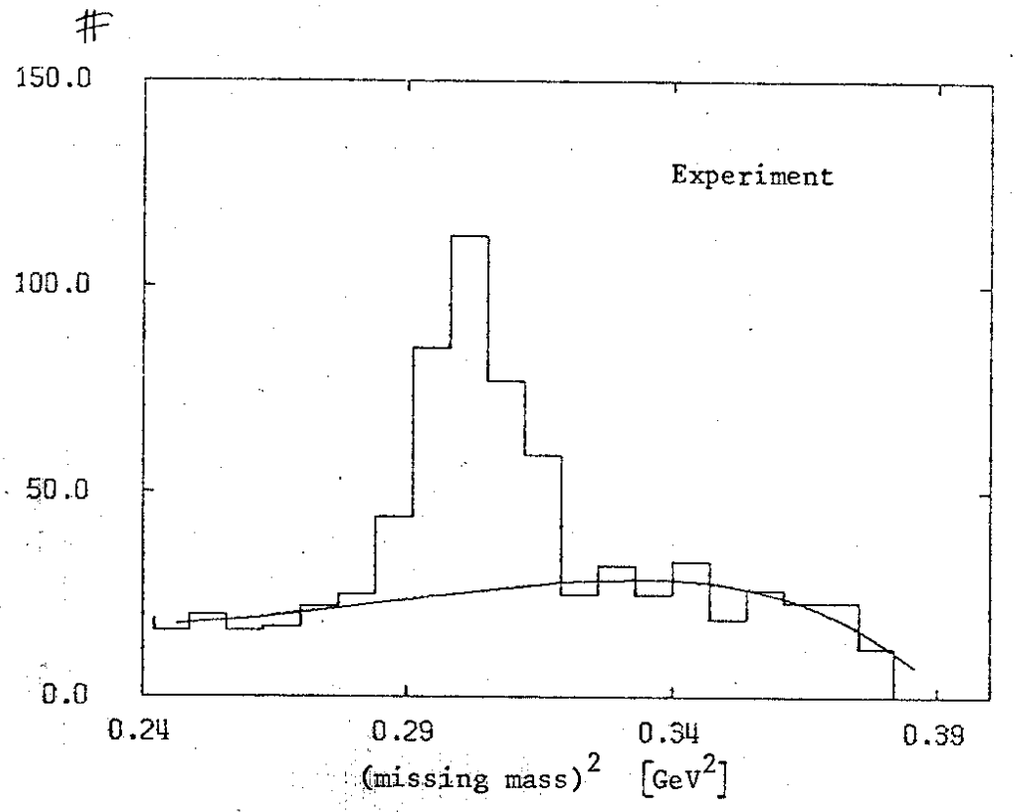

Q**2 = 1 GEV**2, W = 1595 MEV, COS(THX)=-0.3, PHI = 60 DEG.

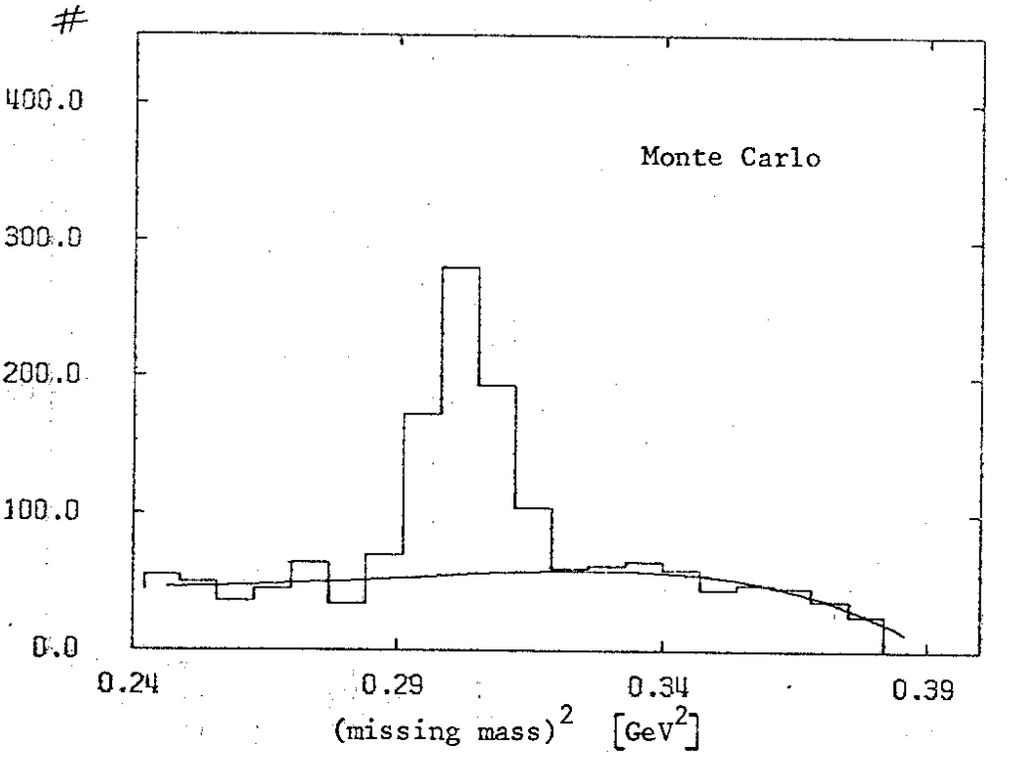

Q**2 = 1 GEV**2, W = 1595 MEV, COS(THX)=-0.3, PHI = 60 DEG.

Fig. 5

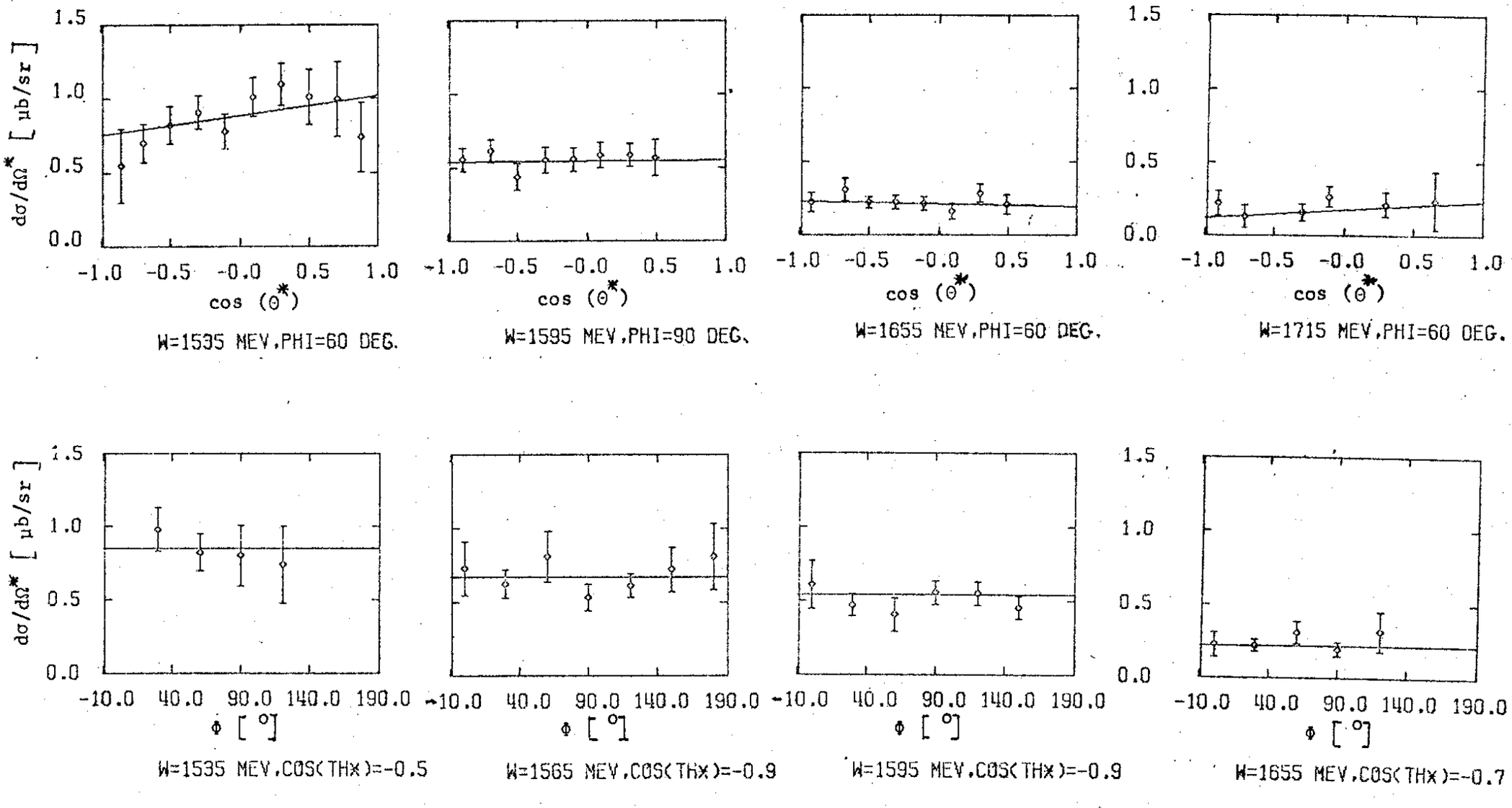

$q^2 = 1\ GeV^2$

Fig. 6

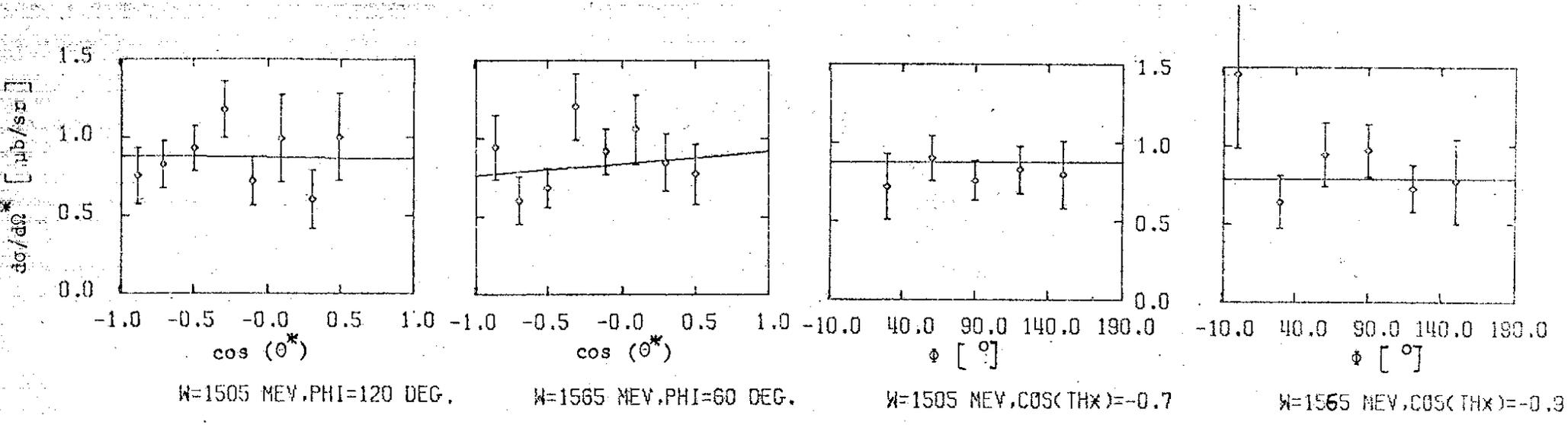

$q^2 = 0.6\ GeV^2$

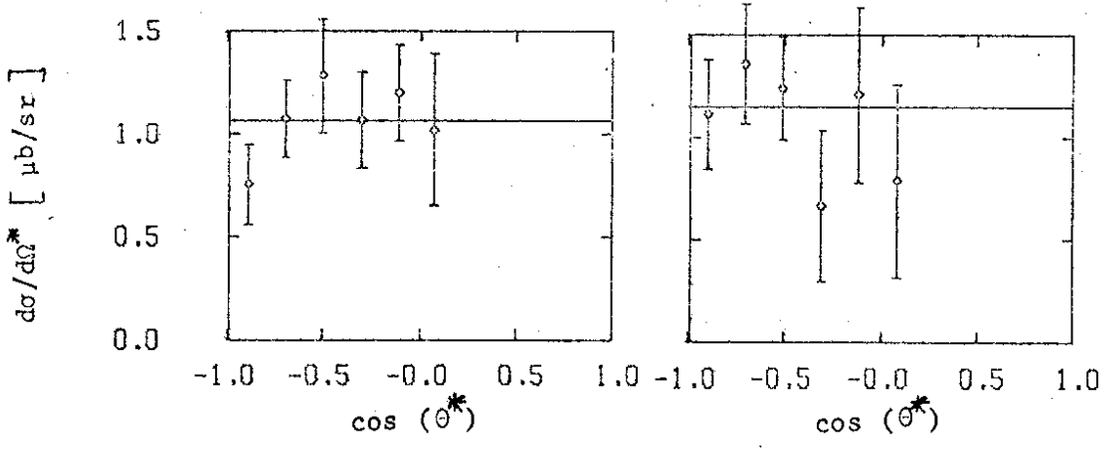

$q^2 = 0.22\ GeV^2$

Fig. 7

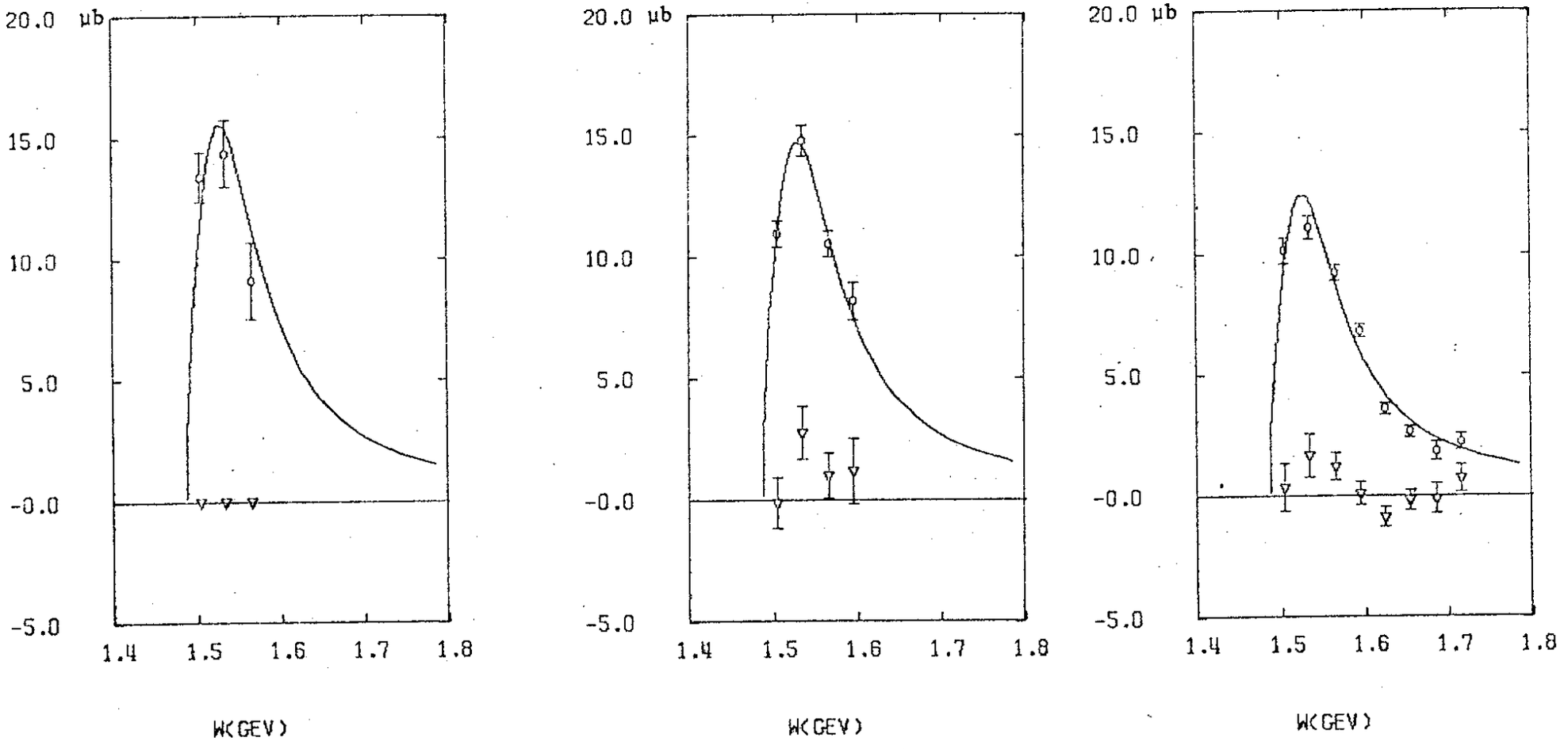

$q^2 = 0.22$ GeV^2 $\qquad$ $q^2 = 0.6$ GeV^2 $\qquad$ $q^2 = 1$ GeV^2

O $\sigma_{tot} = 4\pi\ (A_o + \varepsilon B_o)$ $\qquad$ ▽ $4\pi\ (A_1 + \varepsilon B_1)$

Fig. 8

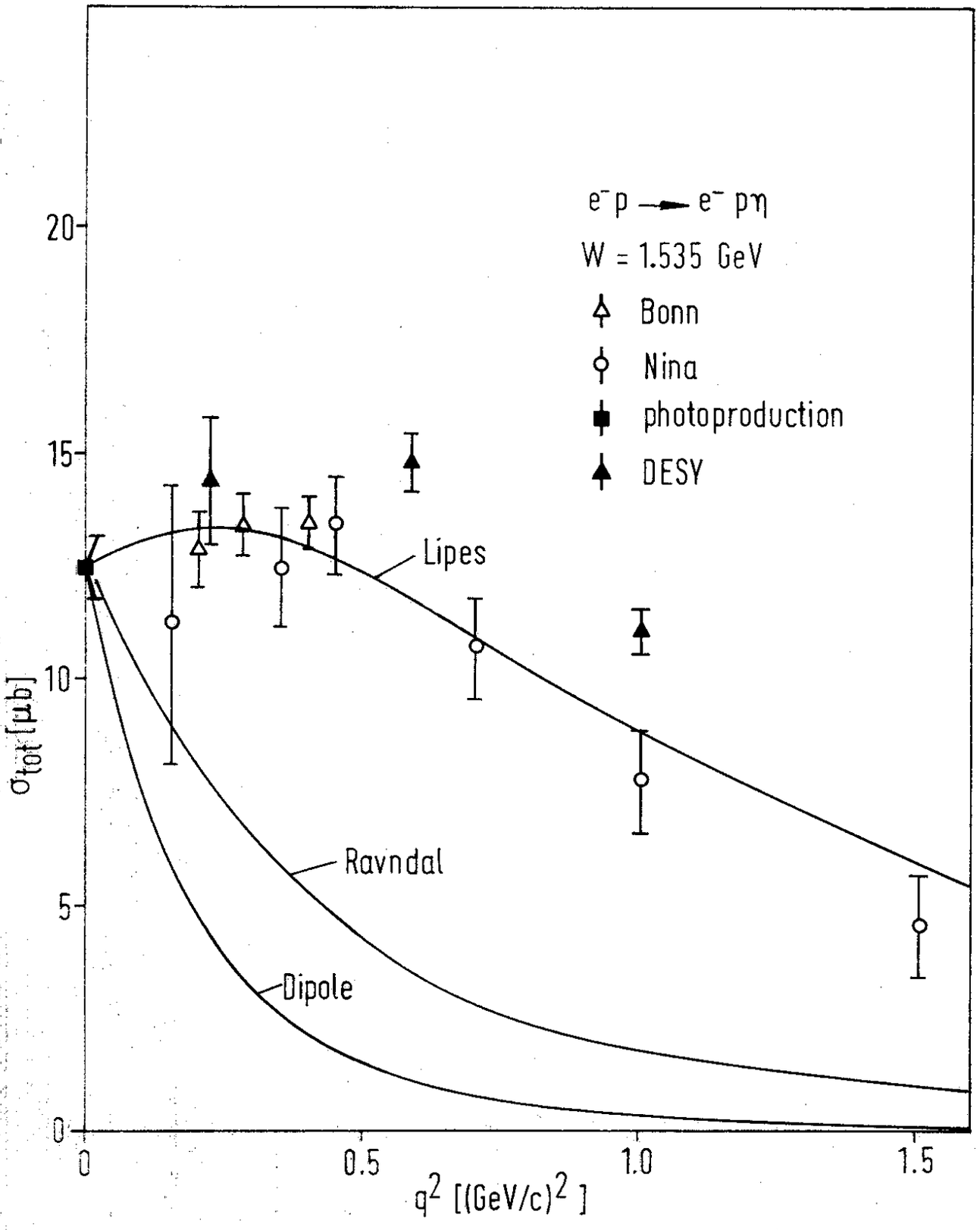
e⁻p → e⁻pη
W = 1.535 GeV
Bonn
Nina
photoproduction
DESY
Lipes
Ravndal
Dipole
σtot [μb]
q² [(GeV/c)²]
0
5
10
15
20
0
0.5
1.0
1.5

Fig. 9